Modelling and Adaptive Control of a Wind Turbine for Smart Grid Applications

Khaled M. Abo-Al-Ez, Raynitchka Tzoneva

Abstract— In smart electrical grids, wind turbines with variable speed are the most attractive choice for high penetration level of wind energy due to their high operation flexibility. Wind turbines are the core component of the wind energy conversion. In this paper, the objectives are to build a realistic wind turbine model for smart grid analysis and simulations, and propose wind power adaptive control algorithms with a mixed criterion of energy maximization and fatigue load minimization during partial and full load regimes. The modelling approach considers wind aerodynamics and tower dynamics. The generator torque set points are calculated based on the wind turbine design values and rotor speed. The blade pitch angle set point is calculated using a proportional feedback control loop during partial load conditions, and a proportional differential control loop during full load conditions. The wind speed is also modelled considering wind turbulence, tower shadow and wind shear. Models and controllers are built in MATLAB Simulink, and simulations are performed using a realistic data of a typical wind turbine. The simulation results show that the proposed models and controllers accurately simulate the expected performance.

Index Terms—**Smart grid, Wind turbine model, pitch control, Torque control, wind speed model**

1 INTRODUCTION

Smart grid provides the platform for a more environment friendly and reliable electrical power system. Wind energy comes at the top of renewable energy sources in smart grids [1].

Wind turbine is the core element of every wind energy conversion system (WECS) project, as it is the wind power extracting device. The modern wind turbines are of variable speed types, in order to maximize power extraction capability [1]. The challenge in WECS control design within smart grids is to realistically model the wind turbine power harvesting process, along with the rotor effective wind speed. This allows accuracy and reliability of the control design to deliver high quality electrical power, with intermittent wind source.

In literature, modelling of the wind turbines has been a crucial issue in the study and analysis of grid integrated WECS. Examples of the used main modelling approaches are presented in [2], [3], and [4]. In [2], the modelling of the wind turbine mainly considered the drive train, while tower bending effects are ignored, and the wind speed is simplified as a sinusoidal function with its mean value increasing linearly. In [3], a fixed speed wind turbine is modelled using connected modules. Although the modelling approach is effective, it does not present the variable speed type. In addition, tower dynamics are neglected and the wind speed model is represented by actual measured wind speed data in the form of time series. In [4], the wind turbine model is simplified to comprise three sub models to simulate the wind turbine operation near the cut-in speed. This simulates the wind turbine performance under only partial loading conditions, and only the wind turbulence effect is added to the wind speed estimated value.

The above mentioned approaches present examples of a wide range of wind turbine models that are used for power system analysis. However, each method adopts some simplifications that neglect important factors, which reduces the accuracy of the model.

This paper introduces a more realistic model that shows the main features of the wind turbine with variable speed, whereby it is considered as a multi-input/multi-output system. The modelling approach takes into account the tower dynamics and the tower shadow effect on the wind speed. In addition, the wind turbulence and shear effects are considered. The proposed adaptive wind turbine power controller is dependent upon the operation mode of the wind turbine (partial or full load). In section 2 of this paper, the control objectives of the wind turbine are specified. In section 3, the mathematical model is presented for each of the wind turbine subsystems. In section 4, power regulation control strategies are proposed based on the wind turbine operating regime. In section 5, wind speed modelling is explained. In section 6, the simulations of the proposed model and controllers are performed in MATLAB Simulink for different wind speed profiles. Finally, the conclusion is given in section 7.

2 CONTROL OBJECTIVES OF WIND TURBINE

Wind turbine control aims at developing power regulation strategies for maximization of harvested power from the wind source and reduction of the mechanical load [5]. Wind turbines with variable speed operation permit continuous variation of rotational speed for maximum aerodynamic power conversion [6]. Operation of the wind turbine has two regimes [7]:

1. Partial load regime.
2. Full load regime.

This work was funded by the THIRP Grant TP 201106110004 'CSAEMS development growth'.

Khaled M. Abo-Al-Ez is with the Centre of Substation Automation and Energy Management Systems (CSAEMS), Cape Peninsula University of Technology, Bellville 7535, South Africa. He is on leave from the Electrical Engineering Dept., Mansoura University, P.O. 35516 Mansoura, Egypt. (e-mail: ezzkhalid@mans.edu.eg).

Raynitchka Tzoneva is the leader of the Centre of Substation Automation and Energy Management Systems (CSAEMS), Cape Peninsula University of Technology, Bellville 7535, South Africa. (e-mail: TzonevaR@cput.ac.za).

Authorized licensed use limited to: Cape Peninsula University of Technology. Downloaded on July 28,2020 at 16:01:26 UTC from IEEE Xplore. Restrictions apply.

Partial load regime takes place in the periods where wind speed is below the rated one, while the full load regime occurs above the rated wind speed. The following discussion focuses on the mathematical formulation of the wind turbine system model showing the input set points, and then it is followed by the controller algorithms design.

3 MATHEMATICAL MODELLING

From the modelling point of view, wind turbine is considered as a multi-input/multi-output system. The approach is to divide this system into interrelated modules. As a result, the set points driving different actuation systems consist of aggregate actions of different controllers. A typical wind turbine with variable speed is composed of five modules representing [7]:

1. Rotor aerodynamic conversion
2. Mechanical system
3. Dynamics of the tower
4. Pitch actuation system
5. Electric conversion

In the following subsections, the mathematical formulation of each module is presented.

3.1 Rotor aerodynamic conversion

Aerodynamic conversion is formulated mathematically by nonlinear equations for the aerodynamic torque (T_a) and the thrust force (F_a) over the rotor blades are as follows [8], [9]:

$$T_a = C_q(\lambda,\theta).\frac{1}{2}\rho_a \pi {r_b}^3.\left(V_{wind} - \dot{S}_{nd}\right)^2 \quad (1)$$

$$F_a = C_a(\lambda,\theta).\frac{1}{2}\rho_a \pi {r_b}^2.\left(V_{wind} - \dot{S}_{nd}\right)^2 \quad (2)$$

$$\lambda = \frac{\Omega_r \,.\, r_b}{(V_w - \dot{S}_{nd})} \quad (3)$$

$$C_q(\lambda,\theta) = \frac{C_p(\lambda,\theta)}{\lambda} \quad (4)$$

Where,
$C_p(\lambda,\theta)$: Power coefficient
$C_q(\lambda,\theta)$: Torque coefficient
$C_a(\lambda,\theta)$: Thrust coefficient
λ : Blade tip to wind speed ratio
θ : Pitch angle (degrees)
r_b : Turbine rotor radius (m)
ρ_a : Air density (kg/m3)
V_{wind} : Wind speed (m/s)
Ω_r : Turbine rotor speed (r.p.m)
S_{nd}: Tower nodding displacement (m)
$\dot{S}_{nd}$: Tower nodding speed (m/s)

3.2 Mechanical system

Rotor speed increases or decreases depending on the difference between the aerodynamic torque, T_a and the electric torque of the generator, T_e. Turbine rotor is rigidly connected to the low speed shaft. The gearbox connects the low speed shaft to the high speed shaft which drives the generator.

With rigid coupling, it is assumed that the rotor speed, Ω_r and the generator speed Ω_g are equal, leading to zero torsional angle. Hence, the rotational losses are ignored. Therefore, the mathematical formulation of the mechanical system is represented by [9]:

$$J_t \,.\, \dot{\Omega}_r = T_a - T_e \quad (5)$$

$$J_t = J_r + {n_{gb}}^2.J_g \quad (6)$$

Where,
J_r : Inertia of rotor (kgm^2)
J_g : Inertia of generator (kgm^2)
J_t : Total inertia of the coupled rotor and generator (kgm^2)
n_{gb} : Gearbox ratio

The stator of the electric generator and the housing of the gearbox are rigidly connected to the frame of the wind turbine nacelle; therefore, a reaction torque is produced. This torque is called the nacelle torque (T_{nac}), and it is calculated as follows [9]:

$$T_{nac} = \frac{n_{gb} \pm 1}{n_{gb}} \,.\, J_g.\dot{\Omega}_r + T_e \quad (7)$$

3.3 Dynamics of the tower

Wind turbine tower is affected by two main forces; the first is the tower nodding force F_{nd} , and the second is the tower naying force F_{ny}. Those tower dynamics are modelled by the following force equations [8], [9]:

$$m_t.\ddot{S}_{nd} + k_t.\dot{S}_{nd} + c_t.S_{nd} = F_{nd} \quad (8)$$

$$m_t.\ddot{S}_{ny} + k_t.\dot{S}_{ny} + c_t.S_{ny} = F_{ny} \quad (9)$$

Where,
F_{nd} : Nodding force (N)
F_{ny} : Naying force (N)
$\ddot{S}_{nd}$: Tower acceleration (m/s^2)
S_{ny}: Tower naying displacement (m)
$\dot{S}_{ny}$: Tower naying Speed (m/s)
$\ddot{S}_{ny}$: Tower naying acceleration (m/s^2)
m_t : Tower top effective mass (tons)
k_t: Structural damping constant
c_t : Spring stiffness constant

Since the foundation of the offshore wind turbine is located in the sea; it is subjected to additional hydrodynamic loading caused by waves and sea currents [10]. Therefore, with offshore wind turbines, the nodding force $F_{nd(offshore)}$ is composed of the thrust force F_a and the hydrodynamic nodding force F_{nd}^{hyd} as follows [9]:

$$F_{nd(offshore)} = F_a + F_{nd}^{hyd} \quad (10)$$

$$F_{nd}^{hyd} = \frac{3}{2} \sum_{k=1}^{N_{t,wave}} \left(\frac{x - y_k}{H_t}\right)^{\frac{3}{2}} F_{nd}^{hyd,k} \quad (11)$$

Authorized licensed use limited to: Cape Peninsula University of Technology. Downloaded on July 28,2020 at 16:01:26 UTC from IEEE Xplore. Restrictions apply.

Where,
x : Water depth (m)
y_k : Distance to water surface at the element k (m)
H_t : Tower hub height (m)

The hydrodynamic loading will also induce coupling to the aerodynamic loading seen by the tower and the nacelle [10]. Therefore, in case of offshore wind turbines, the naying force $F_{ny(offshore)}$ is assumed to be composed of the nacelle force F_{nac} and the hydrodynamic naying force as follows [9]:

$$F_{ny(offshore)} = F_{nac} + F_{ny}^{hyd} \tag{12}$$
$$F_{nac} = \frac{3}{2}\frac{T_{nac}}{H_t} \tag{13}$$
$$F_{ny}^{hyd} = \frac{3}{2}\sum_{k=1}^{N_{t,wave}}\left(\frac{x-y_k}{H_t}\right)^{\frac{3}{2}} F_{ny}^{hyd,k} \tag{14}$$

Where,
T_{nac} : The nacelle torque (N.m)

In case of onshore wind turbines, the wind tower foundation is located on the land with the wind turbulence as the only environmental factor; therefore, the hydrodynamic loading is ignored, and the nodding and naying forces are represented by:

$$F_{nd(onshore)} = F_a \tag{15}$$
$$F_{ny(onshore)} = F_{nac} \tag{16}$$

3.4 Pitch actuation system

The pitch speed (u), which is the control input to the pitch actuation system (servomotor) is calculated based on the control algorithm during partial or full load operation. The output of the actuation system is the pitch angle which is applied to the rotor blades for rotor aerodynamic conversion during the wind turbine operating regimes. The pitch actuation system is presented in Laplace domain as follows [9]:

$$\theta(s) = Y_{pt}(s)\, u(s) \tag{17}$$
$$Y_{pt}(s) = \frac{e^{-\left(TD_d^{pt}+TD_d^{col}\right).s}}{\left(\frac{1}{\left(\omega_0^{pt}\right)^2}.s^2+\frac{2.\beta_{pt}}{\omega_0^{pt}}.s+1\right)} \tag{18}$$

Where,
TD_d^{col} : is defined as the conditional delay time to overcome Coulomb friction (ms).
TD_d^{pt} : pitch delay time (ms)
ω_0^{pt} : pitch eigen frequency (rad/s)
β_{pt} : damping rate

3.5 Electric conversion

The electric torque set point (T_e^*) is calculated from the torque/rotor speed curve based on the wind turbine operating regimes. A simplified first order equation is used to represent the overall dynamic behaviour of the electric generator from the set point to actual electric torque. The actual electric torque is calculated as follows [9]:

$$T_e = T_e^* - \tau_{T_e}\dot{T}_e \tag{19}$$

Where,
τ_{T_e}: Time constant (s)

The functional block diagram that represents the interrelated five turbine modules is presented in Fig.1.

4 Power Regulation Control Strategies

The adaptive power regulation control of the wind turbines is composed of two controllers [6]:

1. Pitch controller: for aerodynamic power regulation
2. Generator control: for maximization of the harvested power

Since there are two operating regimes of the wind turbine based on the wind speed; the two controllers are operating during both operating regimes. In each operating regime one of the controllers is dominant and the other is auxiliary as explained in the following subsections.

4.1 Control during a partial load regime

In the operation periods under the rated wind speed or with partial load regime, the generator controller is the dominant controller that maximizes the captured wind power [6]. This is done by adjusting the electric torque set point (T_e^*) in such a way that the optimum tip to wind speed ratio (λ_{opt}) is tracked [7], [11].The extracted aerodynamic power ($P_a^{\lambda_{opt}}$) at the optimum tip to wind speed ratio is [9] :

$$P_a^{\lambda_{opt}} = C_{p,max}(\lambda_{opt},\theta).\ \frac{1}{2}\rho_a\,\pi\,r_b^2.\left(V_{wind}-\dot{S}_{nd}\right)^3 \tag{20}$$

Based on Eq. (2), the aerodynamic torque at optimum tip to wind speed ratio is:

$$T_a^{\lambda_{opt}} = \frac{C_{p,max}(\lambda_{opt},\theta)}{\lambda_{opt}}.\frac{1}{2}\rho_a\,\pi\,r_b^3.\left(V_{wind}-\dot{S}_{nd}\right)^2 \tag{21}$$

Based on Eq. (5), the electrical torque at the optimum tip to wind speed ratio is:

$$T_e^{\lambda_{opt}} = T_a^{\lambda_{opt}} - J_t\,.\dot{\Omega}_r \tag{22}$$

The generator side converter controls the electric torque based on the electric torque/ rotor speed curve of the wind turbine. The torque value under the cut-in speed is zero. Based on the wind speed operating values, the partial load period is divided into three regions:

Authorized licensed use limited to: Cape Peninsula University of Technology. Downloaded on July 28,2020 at 16:01:26 UTC from IEEE Xplore. Restrictions apply.

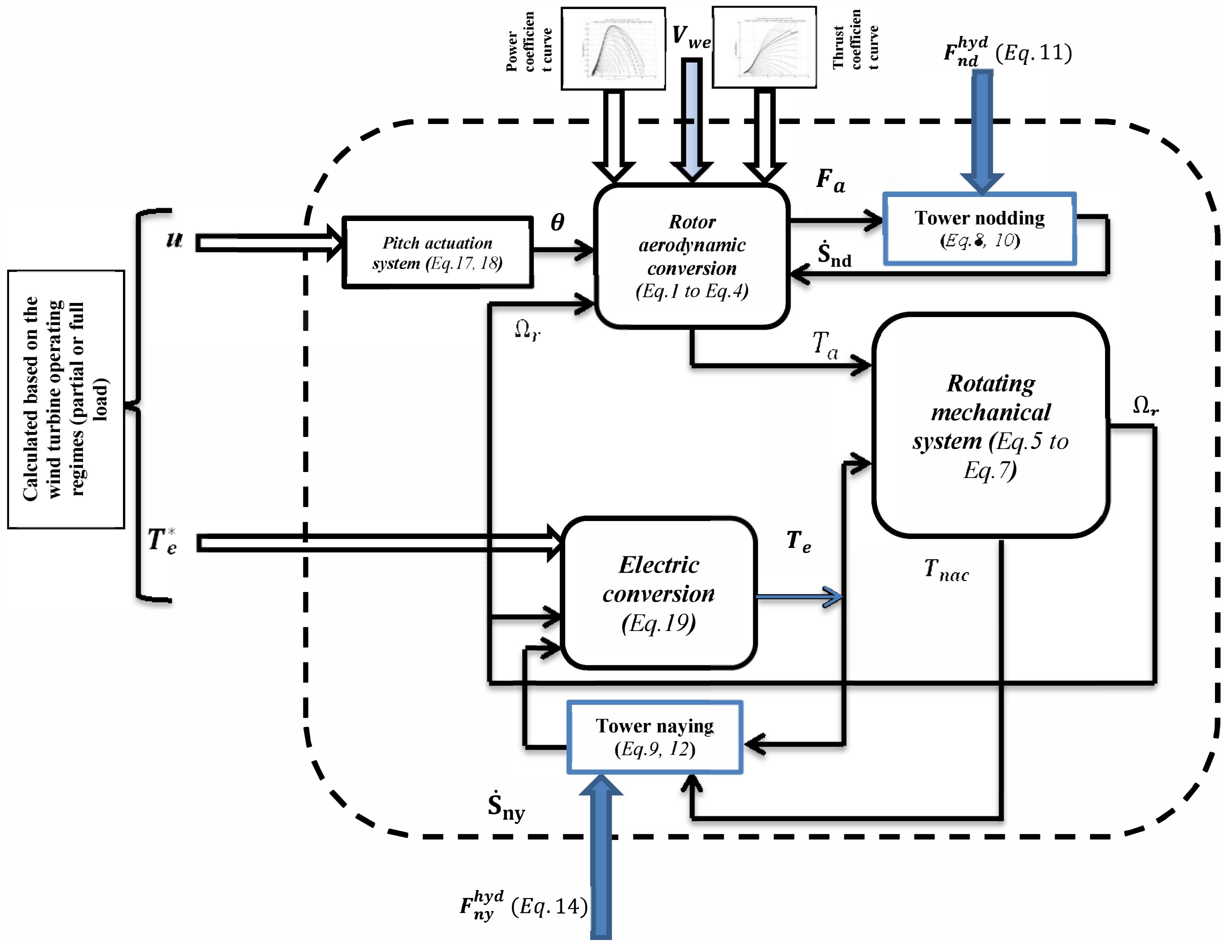

Fig.1 functional block diagram of wind turbine modules

Region1: In this region the partial load regime is starting the optimum tip to wind speed ratio tracking. This region is usually small in terms of time period and it is presented by a steep linear torque /speed curve. The torque set point is calculated by [9]:

$$T^*_{e\,(start)} = \left(\frac{\Omega_r - \Omega_r^{ci}}{\Omega_r^{\lambda_{opt}^{in}} - \Omega_r^{ci}}\right) . T_e^{\lambda_{opt}} . \Omega_r^{\lambda_{opt}^{in}} \tag{23}$$

Where,
Ω_r^{ci}: Rotor speed corresponding to the cut-in wind speed
$\Omega_r^{\lambda_{opt}^{in}}$: Minimum rotor speed with the optimum tip to wind speed ratio

Region 2: In this region the partial load regime is in the region of optimum tip to wind speed ratio. This region is presented by a low order polynomial torque /speed curve. The torque set point is calculated by [9]:

$$T^*_{e\,(\lambda_{opt})} = \sum_{i=1}^{N_{\lambda_{opt}}+1} C_{T_e^{\lambda_{opt}}}(i).\Omega_r^{(i-1)} \tag{24}$$

Where,
$\Omega_r^{\lambda_{opt}^{out}}$: Maximum rotor speed with the optimum tip to wind speed ratio

Region 3: In this region, the partial load regime ends. This region is considered as a transition region between partial load and full load operation. It is presented by a linear transition between the maximum rotor speed with the optimum tip to wind speed ratio ($\Omega_r^{\lambda_{opt}^{out}}$) and the rated rotor speed (Ω_r^{rated}). The torque set point is calculated by [9]:

$$T^*_{e\,(transition)} = T_e^{\lambda_{opt}}.\Omega_r^{\lambda_{opt}^{out}} + \left(\frac{\Omega_r - \Omega_r^{\lambda_{opt}^{out}}}{\Omega_r^{rated} - \Omega_r^{\lambda_{opt}^{out}}}\right).\left(\frac{P_e^{rated}}{\Omega_r^{rated}} - T_e^{\lambda_{opt}}.\Omega_r^{\lambda_{opt}^{out}}\right) \tag{25}$$

Where,
Ω_r^{rated}: Rated rotor speed
P_e^{rated} : The rated electric power (W)

During the partial load regime, the auxiliary control is the pitch angle control. Reference value of the pitch angle is

Authorized licensed use limited to: Cape Peninsula University of Technology. Downloaded on July 28,2020 at 16:01:26 UTC from IEEE Xplore. Restrictions apply.

obtained from a predefined table relating each rotor speed value to its corresponding pitch angle reference value.

The measured pitch angle is compared to the obtained reference value and controlled using a proportional feedback controller (***P**-controller*), which produces the pitch speed (u) control input to the pitch actuation system at partial load conditions.

The proportional gain (K_P^{θ}) is calculated based on a linear model [9]:

$$K_P^{1\theta} \leq \frac{\pi}{4\,.(T_d^{\theta})} \qquad (26)$$

Where,

T_d^{θ} : The delay time = 1.3 s.

4.2 Control during full load regime

In the operation periods above rated wind speed or with full load regime, the pitch angle controller is the dominant controller that limits the extracted wind power to its rated value [6]. Therefore, this controller basically reduces the mechanical loading on the wind turbine. The error in the rotor speed is fed to a Proportional derivative controller (***P-D**-controller*) producing the pitch speed (u) control input to the pitch actuation system at full load conditions. The controller model is:

$$C_{PD}(s) = K_P^f + K_D^f\,.s \qquad (27)$$

The proportional gain, K_P^f , and differential gain,K_D^f are calculated based on [9] as: K_P^f = 1.14 (°/s) / (rad/s), K_D^f = 17.33 (°/s) / (rad/s^2).

5 Wind Speed Modelling

Performance analysis of the WECS models and controllers depends on the wind speed profile as the main external driving signal [12]. Wind is intermittent; therefore wind speed fluctuates in magnitude and direction [13]. Wind speed is modelled based on its effect on the rotor of the wind turbine from two main operation perspectives as:

1. A driving signal.
2. A disturbing signal.

Based on those perspectives, the modelling of the wind speed considers the wind shear, turbulence, and the shadow effect of the tower [14], [15]. The effective wind speed (V_{we}) model includes high frequency and low frequency components [16]. Those two components are dependent upon the rotor azimuth angle (ψ_r) as follows [6], [9]:

$$V_{we} = V_{HF} + V_{LF} \qquad (29)$$

$$V_{HF} = \overline{V}_w \times [1 + v_w^{tur}(\psi r)] \qquad (30)$$

$$V_{LF} = \overline{V}_w \times [1 + v_w^{tur0p}(\psi_r)] \times [v_w^{tower}(\psi_r) + v_w^{shear}(\psi_r)] \qquad (31)$$

$$\psi_r = \int_0^t \Omega_r\,.dt \qquad (32)$$

Where:

v_w^{tur},v_w^{tur0p},v_w^{tower},v_w^{shear} are the normalized wind speed variations with different effects (turbulence, tower shadow, wind shear) respectively, with respect to the mean wind speed $\overline{V}_w$.

6 Simulations and Results Analysis

Dynamic models are developed using MATLAB Simulink software, to represent the overall wind turbine model and the adaptive control strategies. The feedback loops for the adaptive power regulation controllers as modelled in MATLAB are shown in Fig.2. Based on the effective wind speed value, a wind turbine operation regime detector selects the operation regime, hence the required pitch angle controller for either partial load or full load conditions. The system data used for verification of the proposed models and controllers are based on the Dutch wind turbine data presented in [9]. Table.1 summarizes the operational and system data to be used in the simulation.

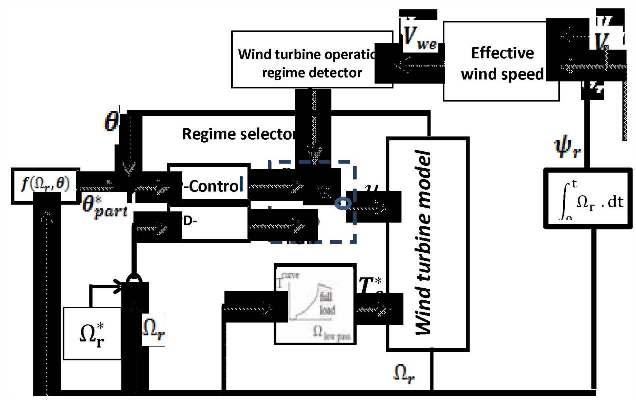

Fig.2. Feedback loops of the adaptive power regulation controllers

Table.1 Operational and system data [9]

Rated electric power P_e^{rated}	2750 kW
Wind speed (rated) V_w^{rated}	12.3 m/s
Rated rotor speed Ω_r^{rated}	15.7 r.p.m or (1.65 rad/s)
Cut in wind speed V_w^{ci}	4 m/s
Cut out wind speed V_w^{co}	25 m/s
Air density ρ_a	1.225 kg/m^3
Rotor blades number	3
Radius of the rotor r_b	46 m
Inertia of the rotor J_r	12.6 * 106 kg.m^2
Inertia of the generator J_g	239 kg.m^2
Hub height H_t	94 m
Starting pitching speed $\dot{\theta}_{start}$	0.5 º s
Full pitch speed $\dot{\theta}_{full}$	4 º s
Max. pitch angle θ_{wt}^{max}	90º
Min. pitch angle θ_{wt}^{min}	- 2.5 º

6.1 Scenario 1: Linear increase of the wind speed

The wind speed changes linearly from 4 m/s. the estimated, uniform, and effective wind speed are shown in Fig.3. The effective wind speed is the driving signal of the turbine model under simulation. Generator power and torque curves are calculated from the simulation model, as shown in Fig 4 and Fig 6, respectively.

Authorized licensed use limited to: Cape Peninsula University of Technology. Downloaded on July 28,2020 at 16:01:26 UTC from IEEE Xplore. Restrictions apply.

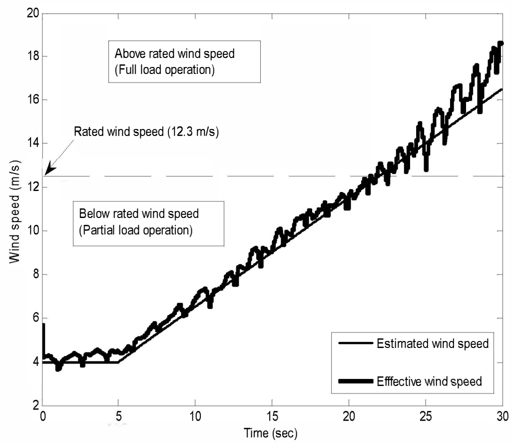

Fig.3. Linear increase of wind speed

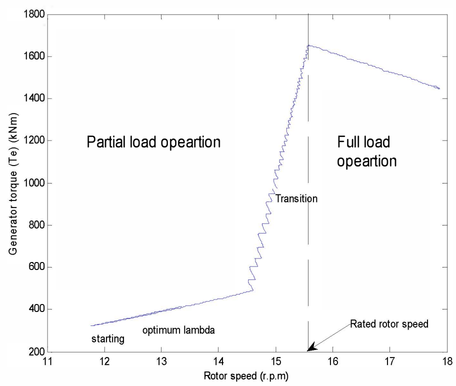

Fig.4 Simulation of generator torque/rotor speed curve

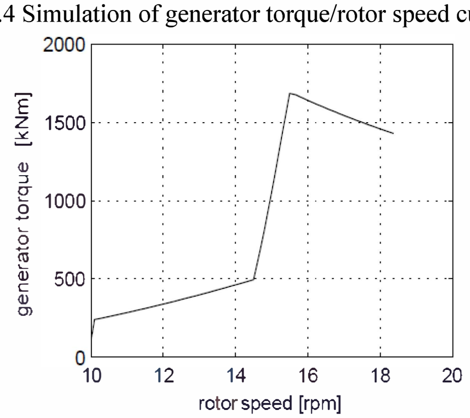

Fig.5 Generator torque/ rotor speed curve as in [9]

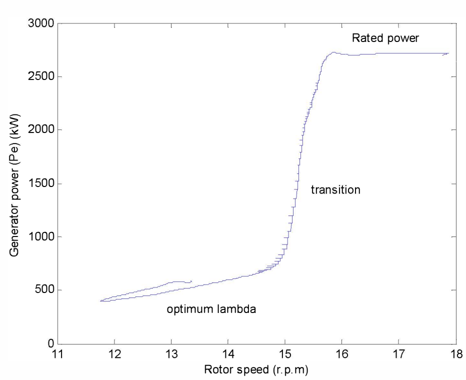

Fig.6 Simulation of generator power/rotor speed curve

Comparison between the simulation torque / rotor speed curve, Fig.4, with the steady sate torque/rotor speed curve obtained in [9], Fig.5, shows that the simulation accurately represents the realistic operating regions of the wind turbine under partial and full load conditions. It should be noted that the starting region is very small compared to the optimum tip to wind speed ratio (optimum lambda) region. During the full load region, the generator torque operation tends to limit the produced electric power to its rated value as shown in Fig.6 of the generator power/ rotor speed curve. This verifies that the proposed wind turbine model and controllers accurately represent the characteristics of a typical variable speed wind turbine under different operating conditions.

6.2 Scenario 2: different mean wind speed values

Having verified that the proposed model and controllers present the operating regions of the wind turbine during partial and full load conditions, it is important to show the power regulation control performance using two different mean wind speeds: (100% , and 160%) of the rated wind speed.

For each mean wind speed the following calculations are obtained from the simulation:

- Effective wind speed (V_{we}) in (m/s) vs. simulation time
- Rotor speed (Ω_r) in (r.p.m) vs. simulation time
- Electric power (P_e) (kW) vs. simulation time
- Generator torque (T_e) (kNm) vs. simulation time
- Pitch angle (θ) in (°) vs. simulation time
- Pitch speed ($\dot{\theta}$) in (°/s) vs. simulation time

6.2.1 Control performance at 100% of the rated wind speed

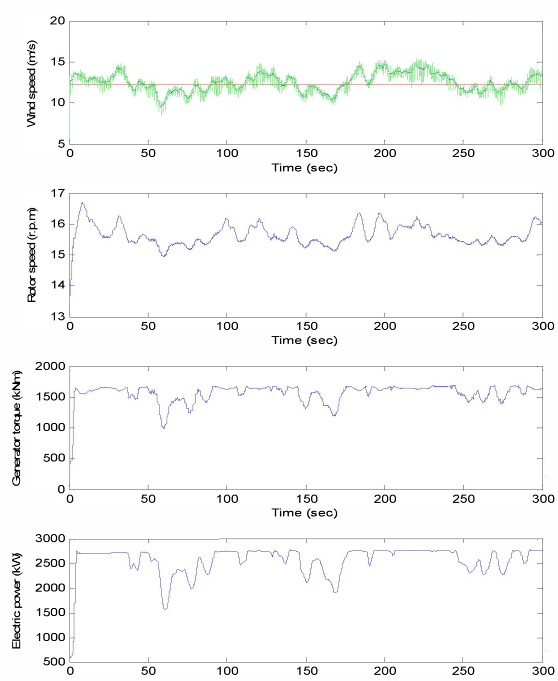

Authorized licensed use limited to: Cape Peninsula University of Technology. Downloaded on July 28,2020 at 16:01:26 UTC from IEEE Xplore. Restrictions apply.

Fig.7 Wind turbine operation curves with 100% rated wind speed

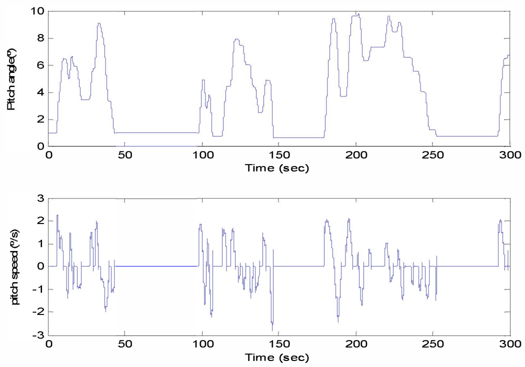

Fig.8 Pitch angle and pitch speed with 100% rated wind speed

The mean power production for the simulation period amounts to 2358kW (85.7% of its rated value). This decrease below the rated value is because of the drop of the wind speed for long time periods during the simulation. During these periods, the pitch angle is adjusted by the controller to (1^o). The generator control is operating at the optimum tip to wind speed ratio. Power production is limited to its rated value for wind speeds above the rated (e.g. this is clear in time periods such as between (194s-240s). Rotor speed mean value is 98% of its rated value.

6.2.2 Control performance at 160% of the rated wind speed (high wind speed)

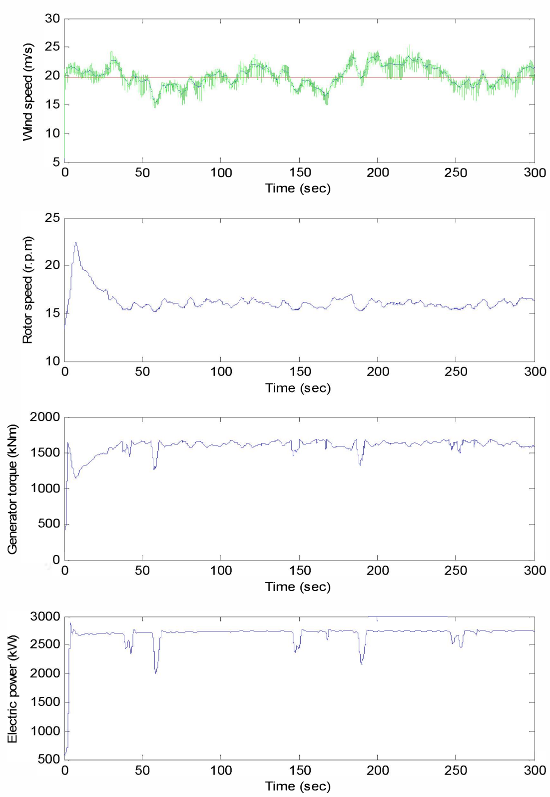

Fig.9 Wind turbine operation curves with 160% rated wind speed

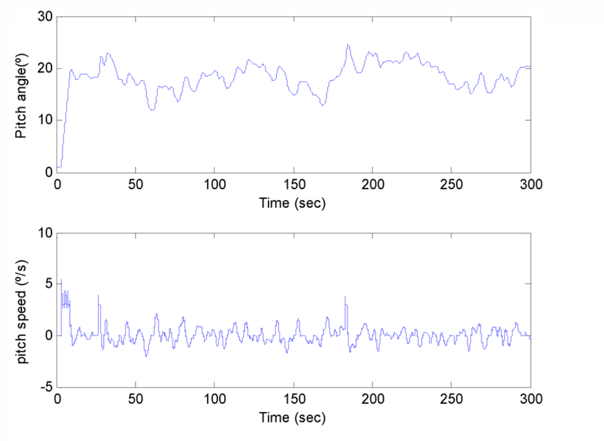

Fig.10 Pitch angle and pitch speed with 160% rated wind speed

The mean power production for the simulation period amounts to 2747kW (99.9% of the rated value). For time periods where wind speed is above the rated one, the power production is limited to its rated value. It can be noticed that at this wind speed level, the pitch angle is varying according to the fluctuations of the wind speed profile as shown in Fig.10.

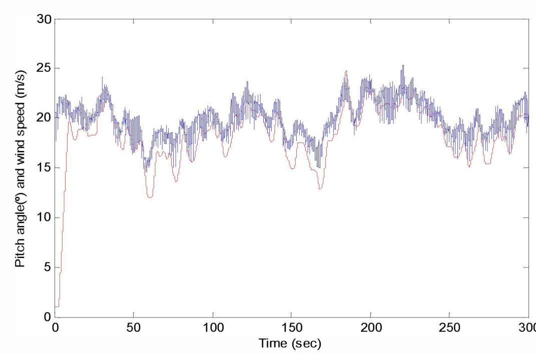

Fig.10 Pitch angle varying according to the wind speed profile for the 160% rated wind speed

6.3 **Discussion of the results**

The first simulation scenario was intended to show the adaptive performance of the power regulation controllers by presenting the relation between the generated electric torque and the rotor speed. The resulting curve showed accurate realistic presentation of the wind turbine torque characteristics below and above rated wind speed when compared to a peer typical curve. The resulting simulation of the electric power curve showed that the controllers are capable of maximum power tracking during partial load conditions, and that they are able to limit the extracted power to its rated value under full load conditions. The second simulation scenario was intended to show the power control performance during rated wind speed operation and during a high wind speed operation, considering the wind speed variations caused by the turbulence, wind shear and tower shadow. With high wind speed, the mean power

Authorized licensed use limited to: Cape Peninsula University of Technology. Downloaded on July 28,2020 at 16:01:26 UTC from IEEE Xplore. Restrictions apply.

production increases as the wind speed profile is above the rated even with wind fluctuations. Also, the blade pitch angle was tracking accurately the wind speed profile.

7 CONCLUSION

This paper developed the mathematical formulation of a realistic wind turbine model for smart grid applications.

The proposed wind power regulation algorithms are determined through the criteria of power maximization during partial load regime and power limitation to the rated value to minimize fatigue load during full load regimes. The modelling approach considered wind aerodynamics and tower dynamics. The simulation results show that the proposed models and controllers accurately simulate the expected performance of a wind turbine with variable speed. The developed models and controllers will be used to study the operation of a grid connected wind turbine generators to analyse different integration scenarios.

REFERENCES

[1] M. Glinkowski, J. Hou, and G. Rackliffe, “Advances in Wind Energy Technologies in the Context of Smart Grid” Proceedings of the IEEE, Vol. 99, No. 6, June 2011.

[2] Y.J. Lin, "Simulating dynamic behavior of a grid-linked wind farm power system in Taiwan", Proceedings of the 12th IEEE Mediterranean Electro technical Conference, 2004.

[3] S. Santoso, H.T. Le, “Fundamental time-domain wind turbine for wind power studies”, Journal of Renewable Energy, Vol.32, Issue 14, November 2007, p.2436-2452.

[4] C. Eisenhut, F. Krug, C. Schram, and B. Klockl, “Wind-Turbine Model for System Simulations Near Cut-In Wind Speed”, IEEE Trans. On Energy Conversion, Vol.22, No.2, June 2007.

[5] C. Jonathan, Y. Creff, "Nonlinear Two Stage Control Strategy of a Wind Turbine for Mechanical Load and Extreme Moment Reduction", Volume 5, Ocean Renewable Energy, 2011.

[6] I. Munteanu, A. Iuliana, B. Nicolaos-Antonio Cutululis, E. Ceang, “Optimal Control of Wind Energy Systems: Towards a Global Approach”, Springer-Verlag London Limited, 2008.

[7] S. Mathew, G. S. Philip, “Advances in Wind Energy Conversion Technology”, Springer-Verlag Berlin Heidelberg, 2011.

[8] H. Ghizlane, J. Chauvin, "Wind speed estimation for wind turbine control", 2012 IEEE International Conference on Control Applications, 2012.

[9] E.L. van der Hooft; P. Schaak; T.G. van Engelen, “Wind Turbine Control Algorithms”, ECN, December 2003.

[10] O. A. Lara, D. C. Gona, E.M. Goytia, G. Adam, “Offshore Wind Energy Generation”, John Wiley & Sons, 2014.

[11] M. G. Sanz. "Power Regulation Strategies for Wind Turbines", Environmental Science and Engineering Journal, 2011.

[12] D. Fu, "Study on linear dynamic model and analysis of operating characteristics of high-power VSCF wind energy conversion system", 2009 World Non-Grid-Connected Wind Power and Energy Conference, 09/2009.

[13] D. Wood, “*Small Wind Turbines: Analysis, Design, and Application*”, Springer Verlag London Limited, 2011.

[14] IEC 61400 standard, “Wind Turbine Generator Systems – Part 1: Safety requirements, IEC 1998.

[15] M. G. Sanz, C. H. Houpis, “*Wind Energy Systems: Control Engineering Design*”, CRC press, 2012.

[16] Shi, Yun-Tao, Qi Kou, De-Hui Sun, Zheng-Xi Li, Shu-Juan Qiao, and Yan-Jiao Hou. "H^{∞} Fault Tolerant Control of WECS Based on the PWA Model", *Energies*, Vol. 7, No.3, p. 1750-1769, 2014.

AUTHORS BIOS AND PHOTOGRAPHS

Khaled M. Abo-Al-Ez received his B.S, M.S, PhD degrees from the Electrical Engineering dept., Mansoura University, Egypt in 2000, 2003, and 2011 respectively. Since March 2015, he is a post doctor fellow at the Centre of Substation Automation and Energy Management Systems, Cape Peninsula University of Technology, South Africa.

Raynitchka Tzoneva has MSc and PhD in Electrical Engineering (control specialization) from the Technical University of Sofia, Bulgaria. Since 1998 she has been a Professor at the department of Electrical Engineering, Cape Peninsula University of Technology, South Africa. She is the leader of the Centre of Substation Automation and Energy Management Systems (CSAEMS) at the Cape Peninsula University of Technology, South Africa. Prof. Tzoneva is a member of the Institute of Electrical and Electronics Engineers (IEEE).

Presenting author: The paper will be presented by Dr. Khaled M. Abo-Al-Ez.

Authorized licensed use limited to: Cape Peninsula University of Technology. Downloaded on July 28,2020 at 16:01:26 UTC from IEEE Xplore. Restrictions apply.